Received: 14 January 2018 | Accepted: 15 May 2018
DOI: 10.1002/hyp.13164

SI STABLE ISOTOPES IN HYDROLOGICAL STUDIES

WILEY

Interpretation of El Niño–Southern Oscillation-related precipitation anomalies in north-western Borneo using isotopic tracers

Naoyuki Kurita[1] | Mayumi Horikawa[2] | Hironari Kanamori[1] | Hatsuki Fujinami[1] | Tomo'omi Kumagai[1,3] | Tomonori Kume[4] | Tetsuzo Yasunari[5]

[1] Institute for Space-Earth Environmental Research (ISEE), Nagoya University, Nagoya, Aichi, Japan

[2] Graduate School of Environmental Studies, Nagoya University, Nagoya, Aichi, Japan

[3] Graduate School of Agricultural and Life Sciences, The University of Tokyo, Tokyo, Japan

[4] School of Forestry and Resource Conservation, National Taiwan University, Taipei, Taiwan

[5] Research Institute for Humanity and Nature, Kyoto, Japan

Correspondence
Naoyuki Kurita, Institute for Space-Earth Environmental Research (ISEE), Nagoya University, Furo-cho, Chikusa-ku, Nagoya, Aichi 464-8601, Japan.
Email: nkurita@nagoya-u.jp

Present Address
Tomonori Kume, Kyushu University Forest, Kyushu University, Fukuoka, Japan

Abstract

We examined rainfall anomalies associated with the El Niño–Southern Oscillation (ENSO) in northern Sarawak, Malaysia, using the oxygen isotopic composition of rainfall. Two precipitation-sampling campaigns were conducted for isotope analysis: (a) at the Lambir Hill National Park (4.2° N, 114.0° E) from July 2004 to October 2006 and (b) at the Gunung Mulu National Park (3.9° N, 114.8° E) from January 2006 to July 2008. The records from these campaigns were merged with a previously published rainfall isotope dataset from Gunung Mulu site to create a 7-year-long record of the oxygen isotopic composition of Sarawak rainfall. The record exhibits clear intraseasonal variations (ISVs) with periods ranging from 10 to 70 days. The ISVs of 10- to 90-day band-pass filtered oxygen isotopic composition are linked to the synoptic-scale precipitation anomalies over the southern South China Sea (SCS). The lead–lag correlation map of precipitation with the filtered oxygen isotope anomalies shows that an anomalous wet condition responsible for the decrease in oxygen isotopic composition appears over the SCS in association with the passage of north-eastward propagation of the boreal summer intraseasonal oscillation (BSISO) in the summer monsoon season. The anomalous wet condition in spring is connected with eastward-propagating Madden–Julian oscillation (MJO), whereas the sustained wet condition in winter is responsible for the occurrence of the Borneo vortex (BV) over the SCS. ENSO modulates the frequency of these synoptic conditions on a seasonal and longer time scale, showing a strong correlation between the seasonal isotopic anomalies and the Southern Oscillation index. We therefore discern, from the significant correlation between the isotope anomalies and area-averaged Sarawak rainfall anomalies ($R = -0.65$, $p < 0.01$), that ENSO-related precipitation anomalies are linked to the seasonal modulation of the BSISO and MJO activity and BV genesis.

1 | INTRODUCTION

Borneo island is situated at the center of the Asian–Australian monsoon region, an area characterized by an asymmetric seasonal transition between the summer south-west monsoon and winter north-east monsoon. On an interannual time scale, the variability of these monsoons is strongly linked to the El Niño–Southern Oscillation (ENSO;e.g., Cook, Anchukaitis, & Buckley, 2010; Wang, Wu, & Lau, 2001). The Borneo rainfall therefore exhibits an interannual variability related to ENSO (e.g., Chang, Wang, Ju, & Li, 2004; Juneng & Tangang, 2005; Salimun, Tangang, Juneng, Behera, & Yu, 2014; Tangang & Juneng, 2004; Tangang et al., 2017). Drought (flood) conditions generally prevail over north-western Borneo during El Niño (La Niña). During the extreme El Niño event of 1997/1998, an unusually severe

drought induced severe effects in various components of the earth system such as the tropical forest ecosystem, regional air pollution, and the global carbon budget (e.g., Danielsen et al., 2009; Fuller, Jessup, & Salim, 2004; Harrison, 2001; Heil & Goldammer, 2001; Koe, Arellano, & McGregor, 2001; Nakagawa et al., 2000; Page, Siegert, Rieley, Boehm, & Jaya, 2002).

ENSO is also well known to affect seasonal rainfall in north-western Borneo. In particular, its influence can be seen most prominently during its mature phase, which corresponds to the Asian winter monsoon season (December to February). Two major comprehensive hypotheses have been proposed to explain the ENSO-related Borneo rainfall variability. One considers the modulation of the diurnal cycle of rainfall by ENSO-induced wind anomalies (Moron, Robertson, & Qian, 2010; Qian, Robertson, & Moron, 2010; Qian, Robertson, & Moron, 2013). Borneo island has a prominent diurnal cycle of precipitation associated with diurnal land–sea breeze circulation (e.g., Kikuchi & Wang, 2008; Yang & Slingo, 2001). Weather types that are more prevalent during El Niño (La Niña) winters tend to disrupt (enhance) the land–sea breeze cycle (Qian et al. 2013). Significant decreases (increases) in the frequency of rainfall events result in negative (positive) rainfall anomalies over Borneo. In the other hypothesis, rainfall anomalies are associated with the variability of the occurrence of extreme precipitation events. A major portion of the heavy rainfall events are produced by synoptic-scale disturbances propagating from the South China Sea (SCS; Chen, Tsay, Yen, & Matsumoto, 2013a). The westerly winds associated with cyclonic flow over the SCS enhance moisture transport to Borneo, which in turn enhances the diurnal cycle of the rainfall. The changes in ENSO-induced circulation weaken (intensify) synoptic-scale cyclone activity over the SCS during El Niño (La Niña) winters (Chen, Tsay, Yen, & Matsumoto, 2013b; Tangang et al., 2017). Variability of moisture flux from the SCS leads to changes in extreme events. The changing frequency and changing intensity of precipitation events can both explain the ENSO-related precipitation anomalies over Borneo. It has been a significant challenge, however, to quantitatively assess how each contributes to the precipitation anomalies based on reliable simulations or alternative approaches. The challenge stems chiefly from gaps in our knowledge about the complex interaction between synoptic scale moisture flow, topography, and the diurnal cycle. In this study, we employ a new approach, stable water isotopologues, to elucidate ENSO-related rainfall anomalies. Stable water isotopologues such as HDO and $H_2{}^{18}O$ are suitable tools for identifying a dominant factors controlling the ENSO-related Borneo rainfall anomalies. Their relative concentrations in the tropics are related to integrated convective activity over both time and space. Isotopically depleted water vapor and precipitation are observed when convective activity is sustained or water vapor is transported from a convective active region (e.g., Galewsky & Samuels-Crow, 2015; Lawrence, 2004; Lekshmy, Midhun, Ramesh, & Jani, 2014; Kurita, 2013; Kurita et al., 2011; Moerman et al., 2013; Tremoy et al., 2012; Vimeux, Tremoy, Risi, & Gallaire, 2011). As such, the isotopic concentrations of extreme rainfall events associated with synoptic-scale disturbances are presumably lower than those from local convection systems. In contrast, the concentrations are insensitive to changes in the frequency of rainfall associated with the diurnal cycle. The changes in precipitation frequency may thus inhibit the isotopic variations in association with ENSO. Moerman et al. (2013) presented a 5-year-long daily-based record of the isotope ratio of precipitation in north-western Borneo. Their data showed a relationship between the interannual isotopic variability and ENSO with an anomalous high (low) oxygen isotope ratio during El Niño (La Niña). This ENSO-related variability found in isotopic concentrations supports the hypothesis that extreme rainfall plays a major role. In the present study, we add another two sets of precipitation isotope data observed in north-western Borneo to create a 7-year-long dataset and explore whether the extreme events hypothesis can largely explain the ENSO-related precipitation anomalies. We begin by exploring the dominant driver of the variation of precipitation isotopes at multiple time scales. After identifying the dominant mode of isotopic variability, we explore the key atmospheric processes controlling the identified mode and analyse their atmospheric circulation patterns over Borneo and the surrounding ocean. We then apply the identified processes to explain the ENSO-related precipitation anomalies in north-western Borneo.

2 | DATA AND METHODS

2.1 | Tropical convection controls on the isotope ratio of precipitation

Stable water isotope ratios in water vapor and precipitation in the tropics are modified by the vertical water vapor cycle of convection: vertical water transport, condensation, and reevaporation of rainfall (Figure 1; see Galewsky et al., 2016 for a detailed review). When surface moisture lifted by updraft precipitates, heavier isotopes preferentially concentrate into the precipitation, depleting the remaining vapor in the convective updraft of isotopes. As a consequence, the downdraft and subsidence transport moisture with low isotopic composition to the lower atmosphere. In parallel, the reevaporation of raindrops and diffusive exchange between raindrops and the surrounding vapor decrease the isotopic values further, resulting in the injection of an isotopically depleted vapor into the boundary layer. More intense convective activity leads to more precipitation, which in turn leads to greater depletion of the isotopic content of the boundary layer vapor feeding the ensuing convective system (hereafter, we describe this recycling process associated with convection as "convective recycling"). Stable water isotope ratios in precipitation are therefore seen as indicator of the integrated history of convective activity from windward regions to observation sites (Hoffmann, 1997; Yoshimura, Oki, Ohte, & Kanae, 2003; Vuille, Werner, Bradley, & Keimig, 2005; Kurita, Ichiyanagi, Matsumoto, Yamanaka, & Ohata, 2009; Vimeux et al., 2011; Moerman et al., 2013). In this study, we express the isotopic composition as δ, a normalized difference of isotopic ratio (R) from the isotopic ratio of Vienna Standard Mean Ocean Water (R_{vsmow}): $\delta = \frac{R}{R_{vsmow}} - 1$.

2.2 | Data

Precipitation was sampled daily in two precipitation-sampling campaigns conducted for isotope analysis at local meteorological stations

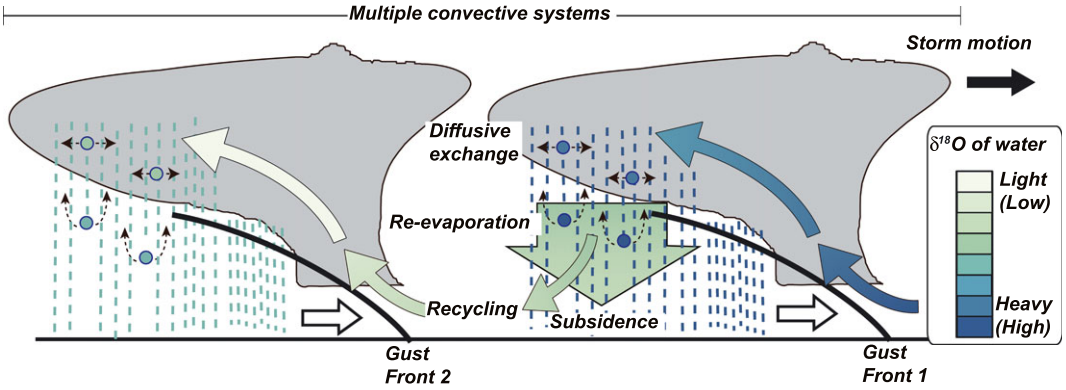

FIGURE 1 Schematic illustration of the evolution of $\delta^{18}O$ in the water vapor feeding the multiple convective systems. The arrows indicate the moisture flow. The colors represent the $\delta^{18}O$ concentrations associated with the color bar

in northern Sarawak, Malaysia: (a) at the Lambir Hill National Park (4.2° N, 114.0° E) from July 2004 to October 2006 and (b) at the Gunung Mulu National Park (3.9° N,114.8° E), 90-km east of the Lambir site, from January 2006 to July 2008 (see Figure 2). The sampling schedule was the same at each station: Rainwater was collected at 8 a.m. local time whenever precipitation had been observed within the previous 24 hr. Plastic sampling bottle (5 L) fitted with 300-mm plastic funnel were installed in an open field to collect the daily precipitation samples. Then the collected samples were transferred to 6-ml glass bottles with polypropylene caps, sealed with parafilm, shipped to the laboratory in Nagoya University in Japan, and analysed for δD and $\delta^{18}O$ using an isotope ratio mass spectrometer (Delta plus XL; Thermo Fisher Scientific) with a water equilibrium device (Nakano Electric Inc.). The measurement precision exceeded ±1.0‰ for δD and ±0.1‰ for $\delta^{18}O$.

A Tropical Rainfall Measuring Mission (TRMM) rainfall product, namely, 3B42 version 7, was used to estimate area-averaged Sarawak precipitation (see Figure 2) and investigate precipitation patterns over Southeast Asia. The TRMM 3B42 product has a 3-hourly temporal resolution and a 0.25° × 0.25° horizontal resolution (Huffman et al. 2007). Original data are available online at http://disc.gsfc.nasa.gov/datacollection/TRMM_3B42_V7.shtml. At daily or longer time scale, the TRMM 3B42 has been found to moderately reproduce observed area averaged precipitation over Sarawak region (Rauniyar, Protat, & Kanamori, 2017).

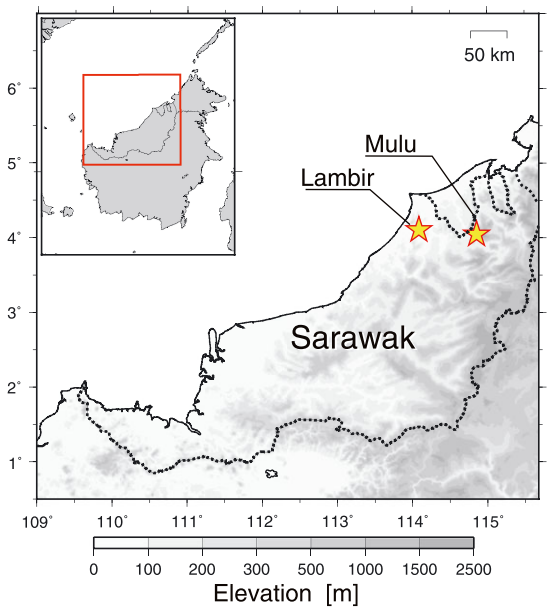

FIGURE 2 Topographic map of the northern Sarawak region in Malaysia around the location of the observation sites. The topography is shaded in gray. The shaded yellow stars mark the Lambir and Mulu stations

Large-scale atmospheric circulation associated with precipitation variability has been investigated using 6-hourly data from a Japanese 55-Year reanalysis (JRA-55) with a horizontal resolution of 1.25° × 1.25° (Ebita et al. 2011). We defined the ENSO phase using the Southern Oscillation index (SOI), the normalized pressure difference between Tahiti and Darwin (Ropelewski & Jones, 1987; available online at http://www.cpc.ncep.noaa.gov/data/indices/soi).

To explore the precipitation variability related to the synoptic-scale disturbances propagating to Sarawak, we focus on intraseasonal and longer time scales, smoothing all of the analysis data with a 10-day running mean filter. The analysis, meanwhile, is based on the ENSO 1-year cycle, which begins in boreal summer (June to August, JJA[0]), strengthens during the autumn (September to November, SON[0]), peaks in the boreal winter (December to February, DJF[0/1]), and weakens in the following spring (March to May, MAM[1]). Years 0 and 1 represent El Niño (La Niña) developing and mature years, respectively. For convenience, Years 0 and 1 are omitted from the text. Anomalies are calculated from seasonal mean during a period with available oxygen isotope data (2004–2011) and then normalized by the standard deviation of the data used for the seasonal mean. Table 1 summarizes the seasonal means and standard deviations employed for the anomaly calculation.

2.3 | A merged 7-year-long dataset of rainfall $\delta^{18}O$ in north-western Borneo

A long-term dataset was created to unveil the mechanism by which ENSO controls the oxygen isotopic composition in precipitation at multiple time scales, from intraseasonal to interannual scales. The observation period at Lambir station overlaps with that at Mulu station in the first half of 2006 (January to June). As shown in Figure 3 a, the temporal (10-day running mean) $\delta^{18}O$ variations at Lambir

TABLE 1 Seasonal means and standard deviations (1σ) of rainfall amount and $\delta^{18}O$ in Sarawak rainfall during a period with available oxygen isotope data (2004–2011)

	Rainfall			$\delta^{18}O$		
Season	Mean mmd^{-1}		1σ mmd $^{-1}$	Mean ‰		1σ ‰
JJA	7.9	±	7.4	−8.4	±	3.0
SON	9.6	±	7.2	−7.9	±	3.4
DJF	12.5	±	9.6	−7.4	±	4.0
MAM	9.4	±	7.2	−7.2	±	3.5

station correspond closely with those at Mulu station, though the individual $\delta^{18}O$ variability is much wider at Mulu than at Lambir. The mean difference in the running mean values between the two stations is 0.22±1.5 ‰ during the overlapping period. Coincidentally, Moerman et al. (2013) have reported a 5-year record of the $\delta^{18}O$ collected at a different site in the Gunung Mulu National Park from July 2006 to May 2011 (available online at WISER database: http://www-naweb.iaea.org/napc/ih/IHS_resources_isohis.html). A part of their observation period also coincides with our Mulu observation (July 2006 to July 2008). A comparison of individual daily rainfall $\delta^{18}O$ shows good agreement between the two Mulu sites (see Figure 3a). The mean difference between our values from this study and the values from Moerman et al. (2013) is −0.20 ± 0.8‰ (N = 309), with first and third quartiles (Q1 and Q3) of −0.46 and 0.12, respectively. Given the close match between the temporal variations of $\delta^{18}O$ from the three stations, we merged these data into a single rainfall $\delta^{18}O$ dataset in north-western Borneo. We calculated the daily average $\delta^{18}O$ between the three stations during the overlapping period and smoothed the data with a 10-day running mean filter. Anomalies are calculated by a method similar to that used to calculate precipitation anomalies. Table 1 summarized the seasonal means and standard deviations for this calculation as well. We then obtained intraseasonal and seasonal-to-interannual anomalies by, respectively, applying band-pass (10- to 90-day) and low-pass (90-day) filters using a Lanczos filter with 121 weights (Figure 4).

A spectral analysis was carried out on smoothed Sarawak rainfall $\delta^{18}O$ dataset. The REDFIT program was used to compute the Fourier analysis and confidence level calculation of the dataset. The significance of the REDFIT power spectrum was assessed by red-noise spectral using Monte Carlo simulation analysis (Schulz & Mudelsee, 2002).

3 | RESULTS AND DISCUSSION

3.1 | Mechanism of intraseasonal rainfall $\delta^{18}O$ variability

Figure 3a exhibits the multiyear time series of northern Sarawak rainfall $\delta^{18}O$ from 2004 to 2011. Moerman et al. (2013) reported that an annual cycle of $\delta^{18}O$ at Mulu reflects a weak seasonal cycle and dominant intraseasonal variability (ISV). As seen in Figure 3a, more than 5 ‰ negative excursions of $\delta^{18}O$ associated with the ISV similarly appear in the data from both the Lambir and Mulu sites. A spectral analysis of the merged $\delta^{18}O$ time series demonstrates a dominant cycle spanning a period of between 10 and 70 days (Figure 5). This is consistent with the pronounced ISV modes of Sarawak rainfall, which span periods of 20 to 90 days (Kanamori, Yasunari, & Kuraji, 2013; Rauniyar et al., 2017). Moerman et al. (2013) also found that the day-to-day $\delta^{18}O$ variability was correlated more strongly with the TRMM rainfall retrieved within the 2.5° × 2.5° longitude/latitude box than with the local precipitation. The correlation, moreover, is even higher on a submonthly mean and longer time scale. These findings imply that the negative excursions of $\delta^{18}O$ may correspond to the ISV of rainfall over the Sarawak area (see Figure 2). Here, we extracted the intraseasonal component of area-averaged Sarawak rainfall using a 10- to 90-day band-pass filter to explore how the Sarawak rainfall and $\delta^{18}O$ anomalies closely correlate on an intraseasonal time scale (Figure 6). As expected, the cross-correlation shows a robust relationship between Sarawak rainfall anomalies and $\delta^{18}O$ anomalies on an intraseasonal time scale, though the Sarawak rainfall anomalies precede the minimum peak of $\delta^{18}O$ anomalies for 5 days (R = −0.41,

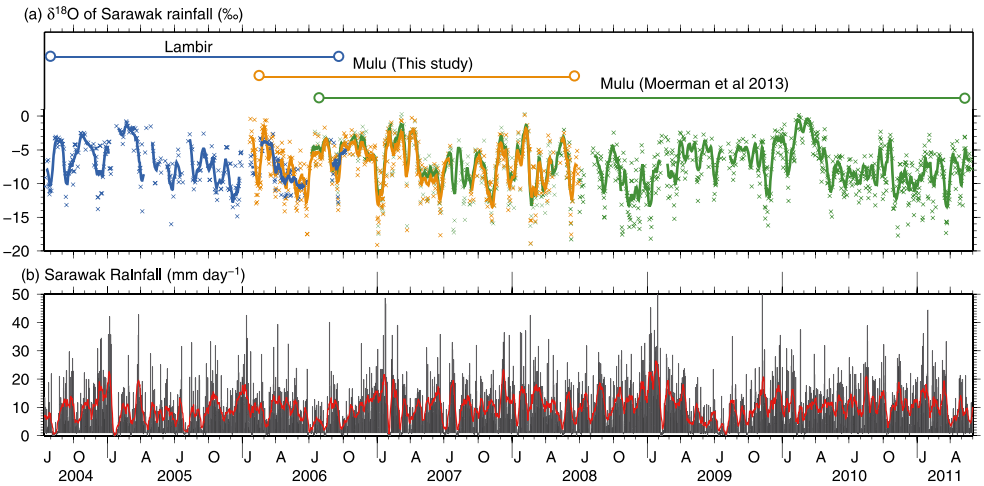

FIGURE 3 (a) Time evolution of $\delta^{18}O$ in precipitation at the Lambir site from July 2004 to September 2006 (blue) and the Mulu site from January 2006 to June 2008 (orange), in northern Sarawak, Malaysia. The green crosses plot data from daily-based Mulu rainfall (from June 2006 to May 2011) reported by Moerman et al. (2013). Each line represents the 10-day running mean of $\delta^{18}O$. (b) Same as (a), but for the area averaged rainfall over Sarawak shown in Figure 1. The red line plots the 10-day running mean of Sarawak rainfall

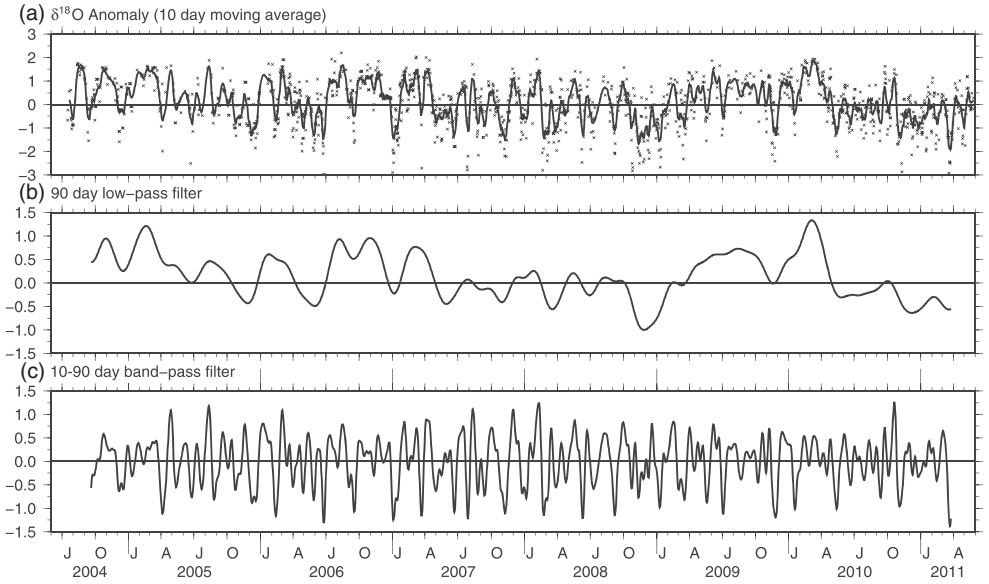

FIGURE 4 A merged 7-year record of rainfall $\delta^{18}O$ between three sites over the period from June 2004 to May 2011. (a) 10-day running mean of $\delta^{18}O$ anomaly normalized by standard deviation. (b) Same as (a), but for 90-day low-pass filtered $\delta^{18}O$. (c) Same as (a), but for 10- to 90-day band-pass filtered $\delta^{18}O$

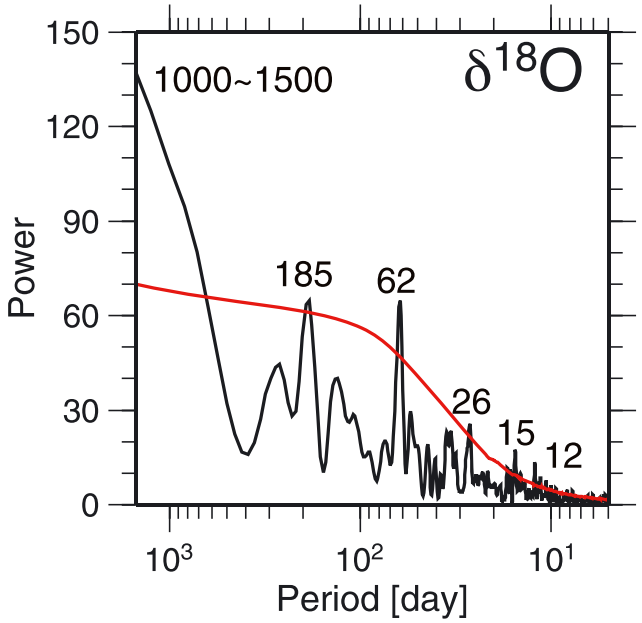

FIGURE 5 The power spectrum of the merged $\delta^{18}O$ record computed using the Lomb–Scargle Fourier transform. The red line plots the 90% confidence intervals assuming a red noise model

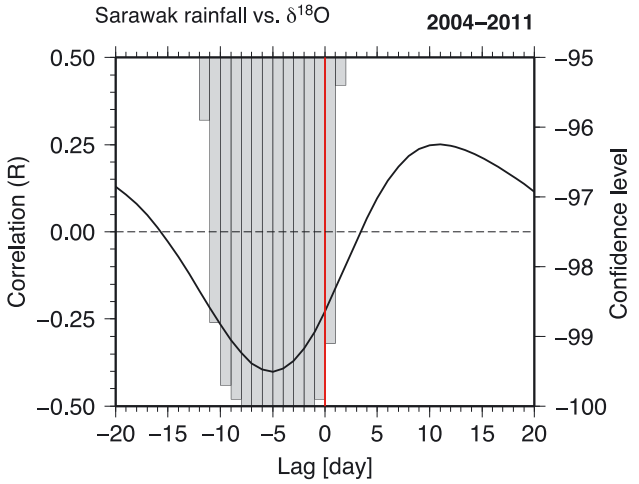

FIGURE 6 Cross-correlation of 10- to 90-day band-pass filtered $\delta^{18}O$ and Sarawak rainfall anomalies (solid line). The gray bars represent confidence intervals

$p < 0.01$). A similar result was reported for local precipitation: Anomalously high local Mulu rainfall appeared for 4 days before the minimum rainfall $\delta^{18}O$ and dropped abruptly to below the long-term average rate after reaching a minimum peak of it (Moerman et al. 2013). Altogether, these results demonstrate that the $\delta^{18}O$ variability is strongly affected by common constraint controls on the Sarawak rainfall variability on an intraseasonal time scale. We speculate that $\delta^{18}O$ depletions occur with a time lag of 5 days after reaching the active phase of the ISV of Sarawak rainfall.

Figures 7 and 8 show the lead–lag correlation of TRMM rainfall anomalies with respect to $\delta^{18}O$ anomalies, on an intraseasonal time scale for each season from 2004 to 2011. A large negative correlation migrating from the Bay of Bengal to the Maritime Continent (MC) can be commonly seen in all seasons except for winter. A negative (positive) correlation indicates that $\delta^{18}O$ anomalies of Sarawak rainfall are negatively correlated with positive (negative) anomalies in the rainfall amounts. The ISV of $\delta^{18}O$ thus seems to be linked to the tropical intraseasonal oscillation (ISO), which appears as a global-scale eastward propagation of large-scale organized convective systems along the equator. The major mode of the ISO is the Madden–Julian oscillation (MJO; Madden & Julian, 1971; Zhang, 2013). The MJO is most active during the boreal winter and spring seasons and weakens

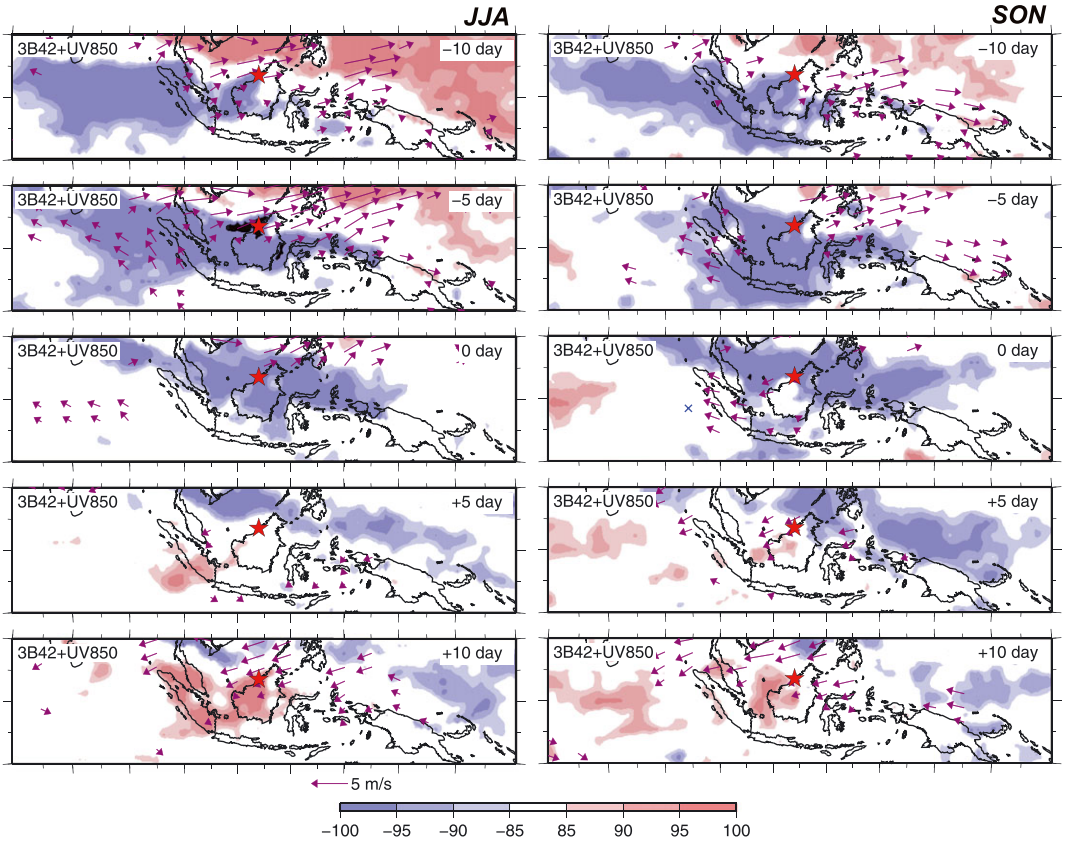

FIGURE 7 Lead–lag correlation patterns of Tropical Rainfall Measuring Mission rainfall and horizontal wind at 850-hPa anomalies based on the 10- to 90-day band-pass filtered $\delta^{18}O$ in the summer monsoon season (JJA and SON) from −10 to 10 days, with Day 0 denoting the center of the wet phase at the South China Sea. The color shading represents the confidence level of the correlation coefficient between Tropical Rainfall Measuring Mission rainfall and $\delta^{18}O$. Blue (red) shading represents a negative (positive) correlation. Only horizontal wind vectors statistically significant at the 90% level are plotted

considerably in summer. The ISO in summer (also known as the boreal summer ISO [BSISO]) shows an off-equatorial component in association with a northward or north-eastward propagation of convection over the Indian Ocean and western Pacific (e.g., Kajikawa, Yasunari, & Wang, 2009; Kikuchi, Wang, & Kajikawa, 2012; Wang, Webster, Kikuchi, Yasunari, & Qi, 2006; Yasunari, 1979). In the patterns observed in the summer south-west monsoon season (JJA and SON) in Figure 7, a large negative correlation appears over the Bay of Bengal and then migrates north-eastward from the MC to the western Pacific Ocean. This propagation feature is consistent with the BSISO. In the winter north-east monsoon season (DJF and MAM), on the other hand, the eastward propagation of the large-scale negative correlation in MAM seems to be connected with the MJO. Although the MJO is the strongest in boreal winter, the negative correlation shows no association with the MJO. The shift of the MJO active center from the north of the equator to the south might explain why no association with the MJO can be found. Furthermore, the stationary negative correlation over the SCS indicates that the ISV of $\delta^{18}O$ is connected with synoptic weather features over the SCS. A stationary closed synoptic-scale cyclonic circulation over the SCS, a phenomenon referred to as the Borneo vortex (BV), is well known to appear in boreal winter (Cheang, 1977; Johnson & Houze, 1987). The BV recurs with a frequency of more than once per month and persists from a few days to a week or longer each time it appears (Chang, Harr, & Chen, 2005; Koseki, Koh, & Teo, 2014). This frequency is much higher than that of the MJO (less than once per month). The impact on the $\delta^{18}O$ variability in association with the MJO thus has a less conspicuous influence compared with that in association with the BV. Now that we are convinced of the close connection between the ISO activity and ISV of $\delta^{18}O$, our next step is to seek a physical explanation for this relationship. The convectively active phase of the ISO with the low $\delta^{18}O$ is much wetter than normal over the SCS. In contrast, the reverse occurs in break phase with the high $\delta^{18}O$. Kanamori et al. (2013) have studied the mechanism by which the ISO influences Sarawak rainfall. In the active phase of the ISO, an enhanced rainfall area distributes over the SCS, in association with the anomalous cyclonic flow centered over south-west coast of Borneo (see their fig. 9a). The westerly winds associated with cyclonic flow over the SCS intensify moisture transport to Sarawak and exert a direct impact on the diurnal cycle of the Sarawak rainfall. The convergence between offshore wind and synoptic-scale westerly wind may trigger convection and enhance rainfall from midnight to morning. This interpretation reasonably explains why the minima of $\delta^{18}O$ occur with a time lag of 5 days after reaching the mature phase of the rainfall over the SCS (Day 0). Since the $\delta^{18}O$ variations in the tropics reflect a cumulative convective recycling process over several days (e.g., Risi, Bony, & Vimeux, 2008; Kurita, 2013), the $\delta^{18}O$ values gradually decrease, whereas active convection is sustained and reaches its lowest value at the end of active phase of the ISO. It takes a time, meanwhile, before the westerly winds transport the water vapor to Sarawak.

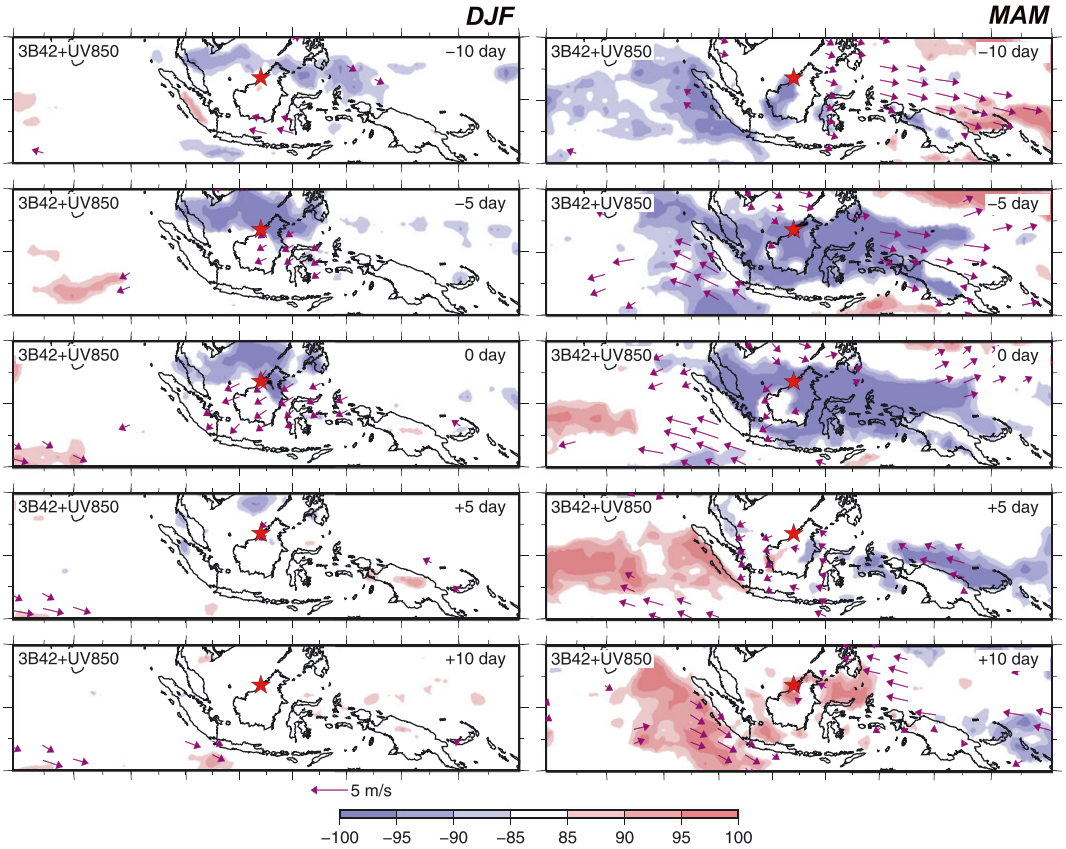

FIGURE 8 Same as Figure 7 but for the winter monsoon season (DJF and MAM)

We thus observed the $\delta^{18}O$ depletions at sites with a time lag of 5 days after reaching active phase of the ISO. Taken together, we can conclude that the ISO activity is the major driver of the ISV of $\delta^{18}O$ in Sarawak rainfall, except in the winter.

In winter, the BV leads to enhanced convection over the southern SCS. Figure 9 shows composite maps of TRMM rainfall and wind patterns at 850 hPa for rainfall events in which significantly lower and higher $\delta^{18}O$ anomalies were observed in Sarawak (anomalies from the winter mean are lower/higher than 1σ [n = 30]). The rainfall events with low $\delta^{18}O$ are characterized by a synoptic pattern with a cyclonic circulation situated off the coast of Sarawak (Figure 9a). Enhanced rainfall areas associated with cyclone distribute over the southern

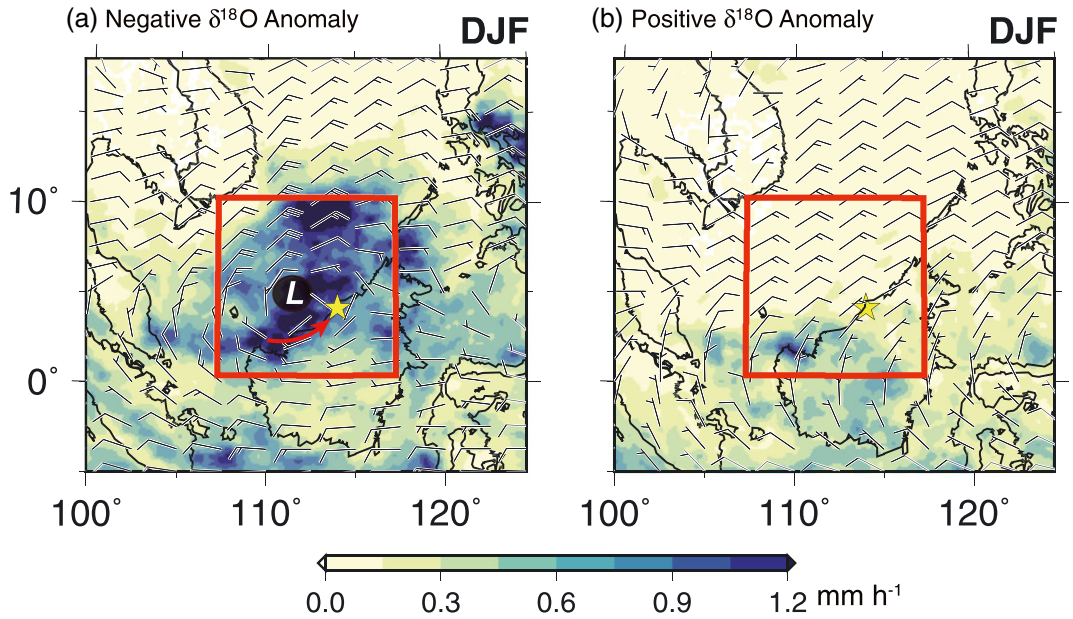

FIGURE 9 Composite maps of Tropical Rainfall Measuring Mission rainfall (mm hr^{-1}) and horizontal winds at 850 hPa (a) in events with negative $\delta^{18}O$ anomalies from the winter average from 2004/2005 to 2010/2011 and in events with positive $\delta^{18}O$ anomalies. The red box encloses the area where the area-averaged vorticity anomaly over the SCS is calculated (see Figure 11)

SCS. Similar to the active phase of the ISO, the westerly winds associated with the cyclone are expected to transport water vapor with low $\delta^{18}O$ values to Sarawak. In events with high $\delta^{18}O$, in contrast, a dry condition prevails over the whole SCS (Figure 9b). The sustained negative correlation over the SCS (see Figure 8) thus identifies the BV as a dominant factor controlling the $\delta^{18}O$ variability in winter.

3.2 | Interpretation of ENSO-related interannual rainfall $\delta^{18}O$ variability

Figure 4b shows a time series of 90-day low-pass filtered $\delta^{18}O$ of northern Sarawak rainfall. The seasonal $\delta^{18}O$ anomalies from the 2004 to 2011 average vary considerably, showing no a regular pattern. These anomalies are linked to the anomalous variances of the 10- to 90-day band-pass filtered $\delta^{18}O$ in all seasons except for winter (Figure 10; $R = -0.65$, $p < 0.01$). Hence, the anomalous intraseasonal events are found to be primarily responsible for the $\delta^{18}O$ variability over seasonal timescales when the ISO activity is a dominant factor controlling the intraseasonal $\delta^{18}O$ variability. In winter, as noted in the previous subsection, the $\delta^{18}O$ variability strongly depends on the BV genesis. The winter anomalies of $\delta^{18}O$ thus show a negative correlation with the seasonal vorticity anomalies over the southern SCS (Figure 11; $R = -0.92$, $p < 0.01$). Given the obvious strength with which the Sarawak rainfall would be affected by the modulation of the ISO and the BV genesis, we find that on a seasonal time scale, the $\delta^{18}O$ anomalies correlate negatively with Sarawak rainfall anomalies without any lag ($R = -0.65$, $p < 0.01$).

Finally, we explore the mechanism for ENSO-related interannual $\delta^{18}O$ variability shown by Moerman et al. (2013). Figure 12a plots a time series of seasonal mean $\delta^{18}O$ anomalies with the seasonal mean SOI and Sarawak rainfall anomalies. A spectral analysis of the $\delta^{18}O$ anomalies exhibits a maximum spectral peak at 3–4 years, a representative of ENSO time scale (Figure 5). On a seasonal timescale, the $\delta^{18}O$

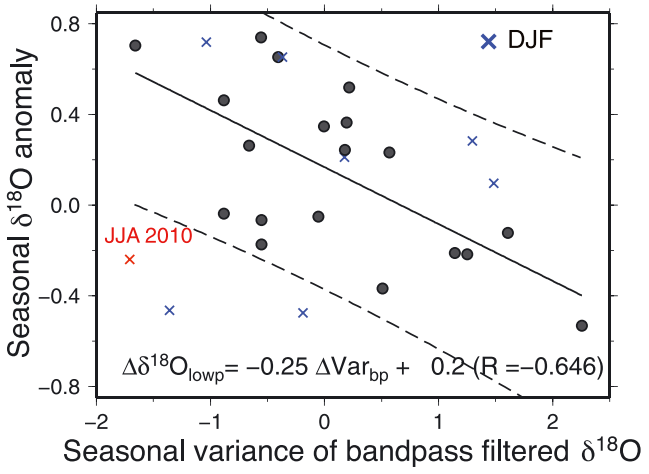

FIGURE 10 Relationship between anomalies of seasonal mean $\delta^{18}O$ and seasonal variances of 10- to 90-day band-pass filtered $\delta^{18}O$. Anomalies for seasonal averaged values are calculated by subtracting the long-term seasonal mean and then dividing by the standard deviation listed in Table 1. The regression line for all season except for winter is shown with the estimation of upper limit of confidence interval (90%). The blue crosses plot the data for the winter season (DJF)

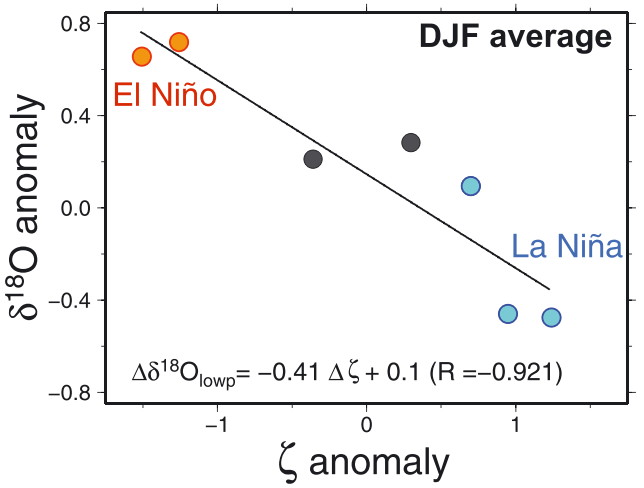

FIGURE 11 Anomalies of winter mean $\delta^{18}O$ of Sarawak rainfall versus area-averaged vorticity (ζ) anomalies over the southern South China Sea (red box in Figure 10). Orange (sky blue) circles represent data from El Niño (La Niña) winter

anomalies show a clear negative correlation with the ENSO index ($R = -0.73$, $p < 0.01$ for SOI). Sarawak rainfall anomalies are also well correlated with the SOI ($R = 0.60$, $p < 0.01$). From this, we speculate that ENSO-related interannual $\delta^{18}O$ variability depends on the seasonal modulation of the ISO and BV genesis. The change in ISO behaviour in response to the ENSO-induced atmospheric circulation anomalies supports this finding. During El Niño, the western subsiding branch of the Walker circulation moving westward leads to the suppressed convection and moisture flux convergence over the MC. Weakened seasonal-mean moisture over the MC prevents the BSISO initiated from the Indian Ocean from passing the MC during the summer monsoon season (Lin and Li, 2008; Liu, Li, Wang, Deng, & Zhang, 2016; Teng & Wang, 2003) and reduces the intensity of the MJO through the feedback effect of convective heating (Chen, Ling, & Li, 2016; Feng, Liu, Chen, & Wang, 2015). The opposite occurs during La Niña. Enhanced moisture over the MC is favourable for the ISO growth. The ISO initiated from the Indian Ocean passes over the wet MC and then propagates northward to the SCS in the summer monsoon season. In the winter monsoon season, the MJO events initiated over the Indian Ocean propagate to the MC and lead to more precipitation over the MC (Moron, Robertson, Qian, & Ghil, 2015; Weaver, Wang, Chen, & Kumar, 2011). The ENSO also strongly modulates the BV genesis (see Figure 11). In El Niño winter, an anomalous low-level anticyclone appears near the Philippine Sea (the Philippine Sea anticyclone: PSAC) due to the Rossby wave response to ENSO (Wang, Wu, & Fu, 2000; Wang & Zhang, 2002). Because of its location along the western edge of the PSAC, the SCS is significantly influenced by southerly wind anomalies during the winter monsoon season, with a weakening of the north-easterly monsoon (e.g., Tangang and Juneng, 2004). During La Niña years, in contrast, cyclonic anomalies develop over the Philippines and thus strengthen the winter monsoon. The weak (strong) winter monsoon therefore reduces (facilitates) the cyclogenesis over the SCS (Chen, Tsay, Yen, & Matsumoto, 2013b). Along with the significant correlation between $\delta^{18}O$ anomalies and Sarawak rainfall anomalies on both seasonal and

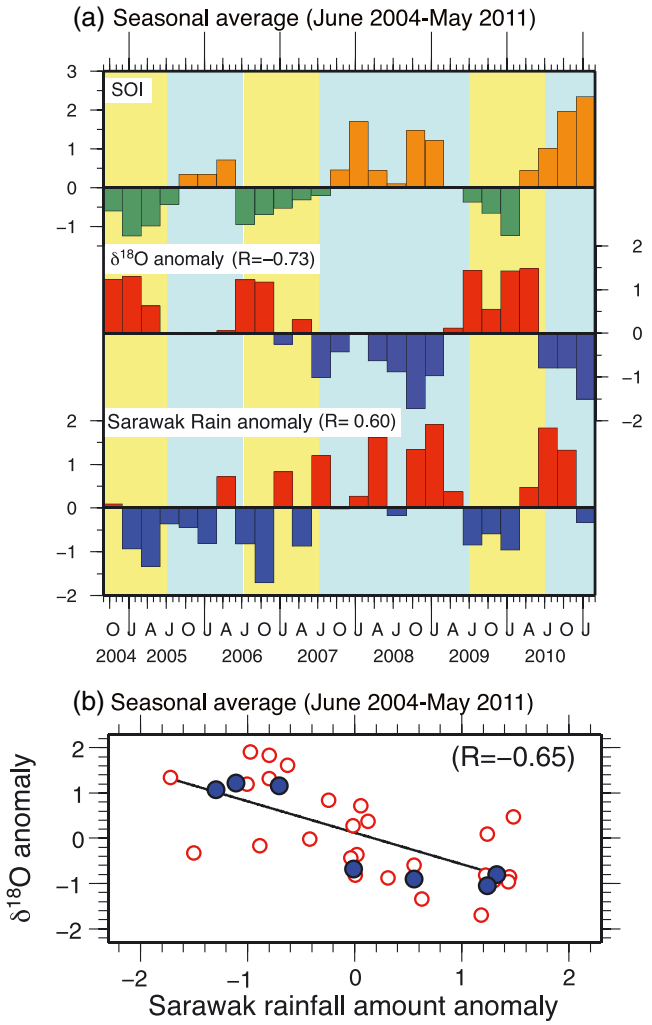

FIGURE 12 (a) Time series of the seasonal mean SOI, $\delta^{18}O$ anomalies, and Sarawak rainfall amount anomalies. Anomalies are seasonal-averaged values calculated by subtracting the long-term seasonal mean and then dividing by the standard deviation. The correlation coefficients between the SOI and each item are also shown. (b) Relationship between seasonal $\delta^{18}O$ and Sarawak rainfall amount anomalies during the whole observation period (July 2004 to May 2011). Blue plots represent the annual means from 2004/2005 to 2010/2011

interannual timescales (Figure 12b; $p < 0.01$), we conclude that ENSO-related interannual Sarawak rainfall variations can be chiefly attributed to changes in the frequency with which extreme events occur.

Intriguingly, this result contradicts the explanation for interannual rainfall variability over the mountains in Java island, which assumes that ENSO-related positive rainfall anomalies are caused by more frequent diurnal cycle (Moron, Robertson, & Qian, 2010; Qian, Robertson, & Moron, 2010). The synoptic-scale disturbances tend to occur frequently near Borneo, whereas the migrations to the Java sea and other Indonesian islands are less frequent (Dang-Quang et al. 2016). The impact of the synoptic-scale disturbances on rainfall anomalies can therefore be presumed to differ among the stations over the MC. Further studies at multiple stations will be necessary to explore the atmospheric processes governing rainfall variability.

4 | CONCLUSIONS

We focused on the oxygen isotopic ratio in Sarawak rainfall to understand the mechanism of ENSO-related precipitation anomalies in Sarawak, north-western Borneo. A merged 7-year record of $\delta^{18}O$ data exhibits a prominent ISV in association with the synoptic-scale disturbances over the SCS. The rapid declines of $\delta^{18}O$ in the summer monsoon correspond to the north-eastward propagation of the BSISO. The large negative $\delta^{18}O$ excursions in winter monsoon season can be attributed to the eastward-propagating ISO (referred to as the MJO) and the occurrence of the BV causing enhanced convection over the southern SCS. The seasonal modulation of the ISO (MJO) activity and BV genesis are primarily responsible for the $\delta^{18}O$ variability over a seasonal or longer timescale. The ENSO-induced atmospheric circulation anomalies are well known to influence the ISO behaviour and BV genesis. The synoptic conditions responsible for the decreases in northern Sarawak rainfall $\delta^{18}O$ occur less (more) frequently during El Niño (La Niña) years than during normal years. These ENSO responses lead to a strong negative correlation between seasonal $\delta^{18}O$ anomalies and the seasonal mean SOI. We can therefore discern, from the significant correlation between $\delta^{18}O$ anomalies and Sarawak rainfall anomalies, that ENSO-related precipitation anomalies are caused by the frequent occurrence of synoptic-scale disturbances over the SCS.

Precipitation isotopologues were intensively monitored by the Japan Agency for Marine-Earth Science and Technology from 2001 to 2010 at six stations in MC (Belgaman et al., 2016; Kurita et al., 2009). The availability of these isotope data will further refine our knowledge of the complex interaction between synoptic-scale moisture flow, topography, and the diurnal cycle over the MC. A long-term record of the isotopic variation in precipitation can also be obtained from paleo-archives such as tree ring cellulose (Schollaen et al. 2013) and stalagmites (Carolin et al., 2013; Carolin et al., 2016; Meckler, Clarkson, Cobb, Sodemann, & Adkins, 2012; Partin, Cobb, Adkins, Clark, & Fernandez, 2007). A retrieval of paleo isotope records from natural archives in Sarawak is very likely to expand our knowledge of the past variability in the frequency of the synoptic-scale disturbances over the southern SCS.

ACKNOWLEDGMENTS

This study was supported by collaborative research program of Hydrospheric Atmospheric Research Center (HyARC) of Nagoya University, entitled "Application of stable isotope for evaluation of multi-scale water cycle processes". The authors gratefully acknowledge members of management committee of analytical system for water isotopes at HyARC of Nagoya University for water isotope analysis and quality control of them. We also thank two anonymous reviewers for constructive comments on the manuscript and editor for their valuable suggestions. The data are available as indicated in Section 2 and otherwise from the authors upon request (nkurita@nagoya-u.jp).

ORCID

Naoyuki Kurita http://orcid.org/0000-0003-1165-0124

REFERENCES

Belgaman, H. A., Ichiyanagi, K., Tanoue, M., Suwarman, R., Yoshimura, K., Mori, S., … Syamsudin, F. (2016). Intraseasonal variability of $\delta^{18}O$ of precipitation over the Indonesian Maritime Continent related to the Madden–Julian oscillation. *SOLA*, *12*(0), 192–197. https://doi.org/10.2151/sola.2016-039

Carolin, S. A., Cobb, K. M., Adkins, J. F., Clark, B., Conroy, J. L., Lejau, S., … Tuen, A. A. (2013). Varied response of western pacific hydrology to climate forcings over the last glacial period. *Science (New York, N.Y.)*, *340*(6140), 1564–1566. https://doi.org/10.1126/science.1233797

Carolin, S. A., Cobb, K. M., Lynch-Stieglitz, J., Moerman, J. W., Partin, J. W., Lejau, S., … Adkins, J. F. (2016). Northern Borneo stalagmite records reveal west pacific hydroclimate across MIS 5 and 6. *Earth Planetary Science Letters*, *439*, 182–193. https://doi.org/10.1016/j.epsl.2016.01.028

Chang, C. P., Harr, P. A., & Chen, H. J. (2005). Synoptic disturbances over the equatorial South China Sea and western Maritime Continent during boreal winter. *Monthly Weather Review*, *133*(3), 489–503. https://doi.org/10.1175/MWR-2868.1

Chang, C. P., Wang, Z., Ju, J., & Li, T. (2004). On the relationship between western Maritime Continent monsoon rainfall and ENSO during northern winter. *Journal of Climate*, *17*(3), 665–672.

Cheang, B. K. (1977). Synoptic features and structures of some equatorial vortices over the South China Sea in the Malaysian region during the winter monsoon. *December 1973, pure and applied geophysics*, *115*(5-6), 1303–1333. https://doi.org/10.1007/BF00874411

Chen, X., Ling, J., & Li, C. (2016). Evolution of the Madden–Julian oscillation in two types of El Niño. *Journal of Climate*, *29*(5), 1919–1934. https://doi.org/10.1175/JCLI-D-15-0486.1

Chen, T.-C., Tsay, J.-D., Yen, M.-C., & Matsumoto, J. (2013a). The winter rainfall of Malaysia. *Journal of Climate*, *26*(3), 936–958. https://doi.org/10.1175/MWR-2868.1

Chen, T.-C., Tsay, J.-D., Yen, M.-C., & Matsumoto, J. (2013b). Interannual variation of the winter rainfall in Malaysia caused by the activity of rain-producing disturbances. *Journal of Climate*, *26*(13), 4630–4648. https://doi.org/10.1175/JCLI-D-12-00367.1

Cook, E. R., Anchukaitis, K. J., & Buckley, B. M. (2010). Asian monsoon failure and megadrought during the last millennium. *Science*, *328*(5977), 486–489. https://doi.org/10.1126/science.1185188

Dang-Quang, N., Renwick, J., & McGregor, J. (2016). On the presence of tropical vortices over the Southeast Asian sea—Maritime Continent region. *Journal of Climate*, *29*, 4793–4800. https://doi.org/10.1175/JCLI-D-14-00468.1

Danielsen, F., Beukema, H., Burgess, N. D., Parish, F., Brühl, C. A., Donald, P. F., … Fitzherbert, E. B. (2009). Biofuel plantations on forested lands: Double jeopardy for biodiversity and climate. *Conservation Biology*, *23*(2), 348–358.

Ebita, A., Kobayashi, S., Ota, Y., Moriya, M., Kumabe, R., Onogi, K., … Ishimizu, T. (2011). The Japanese 55-year reanalysis "JRA-55": An interim report. *SOLA*, *7*, 149–152. https://doi.org/10.2151/sola.2011-038

Feng, J., Liu, P., Chen, W., & Wang, X. (2015). Contrasting Madden–Julian oscillation activity during various stages of EP and CP El Niños. *Atmospheric Science Letters*, *16*(1), 32–37. https://doi.org/10.1002/asl2.516

Fuller, D. O., Jessup, T. C., & Salim, A. (2004). Loss of forest cover in Kalimantan, Indonesia, since the 1997–1998 El Niño. *Conservation Biology*, *18*(1), 249–254.

Galewsky, J., & Samuels-Crow, K. (2015). Summertime moisture transport to the southern south American Altiplano: Constraints from in situ measurements of water vapor isotopic composition. *Journal of Climate*, *28*, 2635–2649. https://doi.org/10.1175/JCLI-D-14-00511.1

Galewsky, J., Steen Larsen, H. C., Field, R. D., Worden, J., Risi, C., & Schneider, M. (2016). Stable isotopes in atmospheric water vapor and applications to the hydrologic cycle. *Reviews of Geophysics*, *54*(4), 809–865. https://doi.org/10.1002/2015RG000512

Harrison, R. D. (2001). Drought and the consequences of El Niño in Borneo: A case study of figs. *Population Ecology*, *43*(1), 63–75. https://doi.org/10.1007/PL00012017

Heil, A., & Goldammer, J. G. (2001). Smoke-haze pollution: A review of the 1997 episode in Southeast Asia. *Regional Environmental Change*, *2*(1), 24–37. https://doi.org/10.1007/s101130100021

Hoffmann, G. (1997). Water isotope modeling in the Asian monsoon region. *Quaternary International*, *37*, 115–128. https://doi.org/10.1016/1040-6182(96)00004-3

Huffman, G. J., Bolvin, D. T., Nelkin, E. J., Wolff, D. B., Adler, R. F., Gu, G., … Stocker, E. F. (2007). The TRMM multisatellite precipitation analysis (TMPA): Quasi-global, multiyear, combined-sensor precipitation estimates at fine scales. *Journal of Hydrometeorology*, *8*(1), 38–55. https://doi.org/10.1175/JHM560.1

Johnson, R. H., & Houze, R. A. J. (1987). Precipitating cloud systems of the Asian monsoon. In C. P. Chang & T. N. Krishnamurti (Eds.), *Monsoon Meteorology* (pp. 298–353). New York: Oxford University Press.

Juneng, L., & Tangang, F. T. (2005). Evolution of ENSO-related rainfall anomalies in Southeast Asia region and its relationship with atmosphere variations in Indo–Pacific sector. *Climate Dynamics*, *25*(4), 337–350. https://doi.org/10.1007/s00382-005-0031-6

Kajikawa, Y., Yasunari, T., & Wang, B. (2009). Decadal change in intraseasonal variability over the South China Sea. *Geophysical Research Letters*, *36*(6), L06,810. https://doi.org/10.1029/2009GL037174

Kanamori, H., Yasunari, T., & Kuraji, K. (2013). Modulation of the diurnal cycle of rainfall associated with the MJO observed by a dense hourly rain gauge network at Sarawak, Borneo. *Journal of Climate*, *26*(13), 4858–4875. https://doi.org/10.1175/JCLI-D-12-00158.1

Kikuchi, K., & Wang, B. (2008). Diurnal precipitation regimes in the global tropics. *Journal of Climate*, *21*(11), 2680–2696. https://doi.org/10.1175/2007JCLI2051.1

Kikuchi, K., Wang, B., & Kajikawa, Y. (2012). Bimodal representation of the tropical intraseasonal oscillation. *Climate Dynamics*, *38*(9), 1989–2000. https://doi.org/10.1007/s00382-011-1159-1

Koe, L. C. C., Arellano, A. F., & McGregor, J. L. (2001). Investigating the haze transport from 1997 biomass burning in Southeast Asia: Its impact upon Singapore. *Atmospheric Environment*, *35*(15), 2723–2734. https://doi.org/10.1016/S1352-2310(00)00395-2

Koseki, S., Koh, T. Y., & Teo, C. K. (2014). Borneo vortex and mesoscale convective rainfall. *Atmospheric Chemistry and Physics*, *14*(9), 4539–4562. https://doi.org/10.5194/acp-14-4539-2014

Kurita, N. (2013). Water isotopic variability in response to mesoscale convective system over the tropical ocean. *Journal of Geophysical Research: Atmospheres*, *118*(18), 10,376–10,390. https://doi.org/10.1002/jgrd.50754

Kurita, N., Ichiyanagi, K., Matsumoto, J., Yamanaka, M. D., & Ohata, T. (2009). The relationship between the isotopic content of precipitation and the precipitation amount in tropical regions. *Journal of Geochemical Exploration*, *102*(3), 113–122. https://doi.org/10.1016/j.gexplo.2009.03.002

Kurita, N., Noone, D., Risi, C., Schmidt, G. A., Yamada, H., & Yoneyama, K. (2011). Intraseasonal isotopic variation associated with the Madden–Julian oscillation. *Journal of Geophysical Research: Atmosphere*, *116*(D24), D24101. https://doi.org/10.1029/2010JD015209

Lawrence, J. R. (2004). Stable isotopic composition of water vapor in the tropics. *Journal of Geophysical Research*, *109*(D6), D06,115. https://doi.org/10.1029/2003JD004046

Lekshmy, P. R., Midhun, M., Ramesh, R., & Jani, R. A. (2014). 18O depletion in monsoon rain relates to large scale organized convection rather than the amount of rainfall. *Scientific Reports*, *4*, 5661. https://doi.org/10.1038/srep05661

Lin, A., & Li, T. (2008). Energy spectrum characteristics of boreal summer intraseasonal oscillations: Climatology and variations during the ENSO developing and decaying phases. *Journal of Climate*, *21*, 6304–6320. https://doi.org/10.1175/2008JCLI2331.1

Liu, F., Li, T., Wang, H., Deng, L., & Zhang, Y. (2016). Modulation of boreal summer intraseasonal oscillations over the western North Pacific by ENSO. *Journal of Climate*, *29*(20), 7189–7201. https://doi.org/10.1175/JCLI-D-15-0831.1

Madden, R. A., & Julian, P. R. (1971). Detection of a 40–50 day oscillation in the zonal wind in the tropical Pacific. *Journal of the Atmospheric Sciences*, *28*(5), 702–708.

Meckler, A. N., Clarkson, M. O., Cobb, K. M., Sodemann, H., & Adkins, J. F. (2012). Interglacial hydroclimate in the tropical West Pacific through the Late Pleistocene. *Science (New York, N.Y.)*, *336*(6086), 1301–1304. https://doi.org/10.1126/science.1218340

Moerman, J. W., Cobb, K. M., Adkins, J. F., Sodemann, H., Clark, B., & Tuen, A. A. (2013). Diurnal to interannual rainfall δ^{18}O variations in northern Borneo driven by regional hydrology. *Earth and Planetary Science Letters*, *369-370*, 108–119. https://doi.org/10.1016/j.epsl.2013.03.014

Moron, V., Robertson, A. W., & Qian, J.-H. (2010). Local versus regional-scale characteristics of monsoon onset and post-onset rainfall over Indonesia. *Climate Dynamics*, *34*(2), 281–299. https://doi.org/10.1007/s00382-009-0547-2

Moron, V., Robertson, A. W., Qian, J.-H., & Ghil, M. (2015). Weather types across the Maritime Continent: From the diurnal cycle to interannual variations. *Frontiers in Environmental Science*, *2*, 163. https://doi.org/10.3389/fenvs.2014.00065

Nakagawa, M., Tanaka, K., Nakashizuka, T., Ohkubo, T., Kato, T., Maeda, T., … Seng, L. H. (2000). Impact of severe drought associated with the 1997–1998 El Niño in a tropical forest in Sarawak. *Journal of Tropical Ecology*, *16*(3), 355–367. https://doi.org/10.1017/s0266467400001450

Page, S. E., Siegert, F., Rieley, J. O., Boehm, H., & Jaya, A. (2002). The amount of carbon released from peat and forest fires in Indonesia during 1997. *Nature*, *420*(6911), 61–65. https://doi.org/10.1038/nature01131

Partin, J. W., Cobb, K. M., Adkins, J. F., Clark, B., & Fernandez, D. P. (2007). Millennial-scale trends in West Pacific warm pool hydrology since the last glacial maximum. *Nature*, *449*(7161), 452–455. https://doi.org/10.1038/nature06164

Qian, J.-H., Robertson, A. W., & Moron, V. (2010). Interactions among ENSO, the monsoon, and diurnal cycle in rainfall variability over Java, Indonesia. *Journal of the Atmospheric Sciences*, *67*(11), 3509–3524. https://doi.org/10.1175/2010JAS3348.1

Qian, J.-H., Robertson, A. W., & Moron, V. (2013). Diurnal cycle in different weather regimes and rainfall variability over Borneo associated with ENSO. *Journal of Climate*, *26*(5), 1772–1790. https://doi.org/10.1175/JCLI-D-12-00178.1

Rauniyar, S. P., Protat, A., & Kanamori, H. (2017). Uncertainties in TRMM-era multisatellite-based tropical rainfall estimates over the maritime continent. *Earth and Space Science*, *4*(5), 275–302. https://doi.org/10.1002/2017EA000279

Risi, C., Bony, S., & Vimeux, F. (2008). Influence of convective processes on the isotopic composition (δ^{18}o and δd) of precipitation and water vapor in the tropics: 2. Physical interpretation of the amount effect. *Journal of Geophysical Research: Atmosphere*, *113*(D19), 3158–12. https://doi.org/10.1029/2008JD009943

Ropelewski, C. F., & Jones, P. D. (1987). An extension of the Tahiti–Darwin southern oscillation index. *Monthly Weather Review*, *115*(9), 2161–2165. https://doi.org/10.1175/1520-0493(1987)115%3C2161: aeotts%3E2.0.co;2

Salimun, E., Tangang, F., Juneng, L., Behera, S. K., & Yu, W. (2014). Differential impacts of conventional El Niño versus El Niño Modoki on Malaysian rainfall anomaly during winter monsoon. *International Journal of Climatology*, *34*(8), 2763–2774. https://doi.org/10.1002/joc.3873

Schollaen, K., Heinrich, I., Neuwirth, B., Krusic, P. J., D'Arrigo, R. D., Karyanto, O., & Helle, G. (2013). Multiple tree-ring chronologies (ring width, δ13c and δ18o) reveal dry and rainy season signals of rainfall in Indonesia. *Quaternary Science Reviews*, *73*, 170–181. https://doi.org/10.1016/j.quascirev.2013.05.018

Schulz, M., & Mudelsee, M. (2002). REDFIT: Estimating red-noise spectra directly from unevenly spaced paleoclimatic time series. *Computers & Geosciences*, *28*(3), 421–426. https://doi.org/10.1016/s0098-3004(01) 00044-9

Tangang, F., Farzanmanesh, R., Mirzaei, A., Supari, E., Jamaluddin, A. F., & Juneng, L. (2017). Salimun characteristics of precipitation extremes in Malaysia associated with El Niño and La Niña events. *International Journal of Climatology*, *112*(2). https://doi.org/10.1002/joc.5032

Tangang, F. T., & Juneng, L. (2004). Mechanisms of Malaysian rainfall anomalies. *Journal of Climate*, *17*(1), 3616–3622. https://doi.org/10.1175/1520-0442(2004)017%3C3616:MOMRA%3E2.0.CO;2

Teng, H., & Wang, B. (2003). Interannual variations of the boreal summer intraseasonal oscillation in the Asian–Pacific region. *Journal of Climate*, *16*(22), 3572–3584. https://doi.org/10.1175/1520-0442(2003)016%3C3572: ivotbs%3E2.0.co;2

Tremoy, G., Vimeux, F., Mayaki, S., Souley, I., Cattani, O., Risi, C., … Oi, M. (2012). A 1-year long δ18o record of water vapor in Niamey (Niger) reveals insightful atmospheric processes at different timescales. *Geophysical Research Letters*, *39*(8). https://doi.org/10.1029/2012GL051298

Vimeux, F., Tremoy, G., Risi, C., & Gallaire, R. (2011). A strong control of the South American SeeSaw on the intra-seasonal variability of the isotopic composition of precipitation in the Bolivian Andes. *Earth and Planetary Science Letters*, *307*(1-2), 47–58. https://doi.org/10.1016/j.epsl.2011.04.031

Vuille, M., Werner, M., Bradley, R. S., & Keimig, F. (2005). Stable isotopes in precipitation in the Asian monsoon region. *Journal of Geophysical Research*, *110*(D23), 28,721–15. https://doi.org/10.1029/2005JD006022

Wang, B., Webster, P., Kikuchi, K., Yasunari, T., & Qi, Y. (2006). Boreal summer quasi-monthly oscillation in the global tropics. *Climate Dynamics*, *27*(7), 661–675. https://doi.org/10.1007/s00382-006-0163-3

Wang, B., Wu, R., & Fu, X. (2000). Pacific–East Asian teleconnection: How does ENSO affect east Asian climate? *Journal of Climate*, *13*(9), 1517–1536.

Wang, B., Wu, R., & Lau, K. M. (2001). Interannual variability of the Asian summer monsoon: Contrasts between the Indian and the western North Pacific–East Asian monsoons. *Journal of Climate*, *14*(20), 4073–4090. https://doi.org/10.1175/1520-0442(2001)014%3C4073: ivotas%3E2.0.co;2

Wang, B., & Zhang, Q. (2002). Pacific–East Asian teleconnection. Part II: How the Philippine Sea anomalous anticyclone is established during El Niño development. *Journal of Climate*, *15*(22), 3252–3265.

Weaver, S. J., Wang, W., Chen, M., & Kumar, A. (2011). Representation of MJO variability in the NCEP climate forecast system. *Journal of Climate*, *24*, 4676–4694. https://doi.org/10.1175/2011JCLI4188.1

Yang, G.-Y., & Slingo, J. (2001). The diurnal cycle in the tropics. *Monthly Weather Review*, *129*(4), 784–801. https://doi.org/10.1175/1520-0493(2001)129%3C0784:TDCITT%3E2.0.CO;2

Yasunari, T. (1979). Cloudiness fluctuations associated with the northern hemisphere summer monsoon. *Journal of the Meteorological Society of Japan*, *57*(3), 227–242.

Yoshimura, K., Oki, T., Ohte, N., & Kanae, S. (2003). A quantitative analysis of short-term 18o variability with a Rayleigh-type isotope circulation model. *Journal of Geophysical Research*, *108*(D), 4647. https://doi.org/10.1029/2003JD003477

Zhang, C. (2013). Madden–Julian oscillation: Bridging weather and climate. *Bulletin of the American Meteorological Society*, *94*(12), 1849–1870. https://doi.org/10.1175/BAMS-D-12-00026.1

How to cite this article: Kurita N, Horikawa M, Kanamori H, et al. Interpretation of El Niño–Southern Oscillation-related precipitation anomalies in north-western Borneo using isotopic tracers. *Hydrological Processes*. 2018;32:2176–2186. https://doi.org/10.1002/hyp.13164